Advances in Geo-Energy Research

Vol. 8, No. 2, p. 76-88, 2023

Original article

Thermal properties of rocks from deep boreholes in Poland in terms of obtaining geothermal energy from enhanced geothermal systems

Krzysztof Labus[1], Małgorzata Labus[1]*, Grzegorz Leśniak[2]

[1]*Institute for Applied Geology, Silesian University of Technology, Gliwice 44-100, Poland*

[2]*Oil and Gas Institute-National Research Institute, Kraków 31-503, Poland*

Keywords:
Geothermal energy
enhanced geothermal systems
thermal conductivity
effusivity
diffusivity

Cited as:
Labus, K., Labus, M., Leśniak, G. Thermal properties of rocks from deep boreholes in Poland in terms of obtaining geothermal energy from enhanced geothermal systems. Advances in Geo-Energy Research, 2023, 8(2): 76-88.
https://doi.org/10.46690/ager.2023.05.02

Abstract:
In the case of unconventional geothermal systems, the thermal conditions are decisive, i.e. heat flux and temperature at a certain depth, and the physical properties of rocks, their susceptibility to fracturing, etc., which should be determined on a local scale. The work carried out was aimed at determining the basic thermal parameters of rocks, i.e.: effusivity, thermal conductivity and diffusivity, basing on tests of samples taken from boreholes, representing selected geothermal structures in Poland. Both high-temperature structures (100-135 °C) recognized up to a depth of about 3,800 m within the Fore-Sudetic Monocline and up to about 3,000 m in the Szczecin Synclinorium and the Leba Elevation, as well as medium-temperature structures (60-90 °C), occurring at depth 2,000-2,500 m (Warszawa Synclinorium, Lublin Synclinorium), were analyzed. Some samples representing low temperature structures (with temperatures below 60 °C), such as Lublin synclinorium and Podlasie-Lublin elevation from depths from about 1,000 to 1,500 m, were also analyzed. The tests of thermal parameters of rocks coupled with simulations showed, that the formations with the highest mean diffusivity and thermal conductivity values are characterized by the largest thermal penetration depth and smallest temperature drop. The research allowed to conclude that among the examined rocks, the Cambrian sandstones of the Leba Elevation and the Zechstein dolomites of the Fore-Sudetic monocline are characterized by the most appropriate parameters from the point of view of obtaining geothermal energy from the enhanced geothermal systems in Poland.

1. Introduction

Earth's heat energy is one of the renewable sources. The potential of geothermal energy is very large. The International Energy Agency estimates that by 2050 electricity from geothermal power plants will account for 3.5% of total electricity production in the world. This means a reduction in carbon dioxide emissions by 800 megatons per year. The agency believes that around 50% of the increase in production will come from geothermal power plants using the concept of hot dry rock (HDR) geothermal energy-exploitation of the heat contained in those regions of the Earth's crust that contain little or no fluids in place (Potter et al., 1974). The use of HDR technology to generate electricity does not cause emissions to the atmosphere or other negative effects on the natural environment. It also increases the share of renewable energy in the total amount of energy produced, which is in line with specific national programs in Central Europe, including Poland, to reduce the emission intensity of the economy. So far, mainly the geothermal energy from shallow geothermal waters (hydrothermal resources) is used in Poland, but research is being carried out to identify also the HDR resources. Every year there are more and more power plants using the heat deposits stored in the interior of the Earth. However, the existing solutions assume the use of heat stored at a depth of up to 4,000 m.

*Corresponding author.
E-mail address: krzysztof.labus@polsl.pl (K. Labus); malgorzata.labus@polsl.pl (M. Labus); lesniak@inig.pl (G. Leśniak).

Yandy Scientific Press

Received February 14, 2023; revised March 20, 2023; accepted April 1, 2023; available online April 8, 2023.

The HDR heat accumulated in the greater depths of the rock mass (mostly between 3,000 and 6,000 m) can be exploited using enhanced geothermal system (EGS). The HDR resources are not connected to either water or steam, but to heat of hot dry or hardly dry rocks (Brown et al., 2012), therefore in an EGS fluid circulation must be stimulated artificially (Boden, 2017).

HDR geothermal technology enables the use of the heat of the Earth's interior in areas without thermal fluids, mainly in the aspect of electricity production in binary systems. For the effective operation of such systems, the temperature of the rock mass above 100 °C is required (Bujakowski et al., 2016).

In Poland, research on geothermal potential has been carried out since the 1980s. From 1990 to 2013, Geothermal Atlases have been developed and published, which show good recognition of geothermal waters in Poland (Górecki et al., 2015; Tomaszewska et al., 2018; Sowiżdżał et al., 2020). Nevertheless, Poland is characterized rather by low-temperature geothermal resources. Sowiżdżał et al. (2020), provide a detailed description of individual geological provinces in Poland in terms of their hydrogeothermal potential.

From the HDR energy point of view, repurposing exploration or abandoned oil and gas wells to geothermal wells can often be a viable option (Kepinska, 2003; Bujakowski et al., 2020; Cui et al., 2021; Santos et al., 2022). In Poland, only 254 wells are 4,000 m or more deep, which accounts for 3% of the total number of deep wells. The suitability of a given borehole for geothermal purposes results from its location within individual geological units, as well as from the technical possibilities of its reconstruction and adaptation to new purposes. Bujakowski et al. (2020) indicate however that even assuming that only a small percentage of extant wells would be suitable for reconstruction, it is enough to consider such a possibility, especially for economic and environmental reasons. Worldwide experience in the use of geothermal energy shows that the site characteristics remain a key factor in the success of HDR development. In most HDR/EGS projects in the world, granite is the reservoir rock for closed geothermal systems, less common are solutions using the energy of hot dry sedimentary and volcanic rocks. In order to identify geological structures in Poland useful for the HDR or EGS technology, a project entitled: "Assessment of potential, heat balance and prospective geological structures for the needs of closed geothermal systems (Hot Dry Rocks) in Poland" was implemented (Wójcicki et al., 2013). From a geological point of view, the best suited for HDR development are mostly crystalline rocks, which occur at depths of 3-5 km. Especially good geological conditions in this respect prevail in the Sudetes, where massifs of igneous rocks of appropriate sizes occur directly on the surface or under the overburden of small thicknesses (Bujakowski et al., 2016).

Research conducted in the USA (Tester, 2006) also shows that some of HDR resources are associated with sedimentary rocks, which due to the depth of deposition are characterized by homogeneity of composition, as in the case of granites, but also by internal porosity and permeability (K). The location is usually chosen based on the thermal gradient analysis of the site. Due to the presence of certain amounts of water in sedimentary rocks, they are also included in the Enhanced Geothermal Systems. A number of projects around the world concern the possibility of using the energy stored in (almost) dry, hot sedimentary rocks. An example of such a project is the Limestone Coast Geothermal Project implemented in Australia, which involves the use of geothermal energy of hot sedimentary basins. European examples of using the potential of sedimentary rocks in EGS systems can be found in Germany, where two geothermal projects: Groß Schönebeck and Landau use (among others) the heat of sedimentary rocks (Huenges, 2010). This applies in particular to the Landau project, which combines the use of hydrogeothermal resources with EGS technology.

In Poland, the prospective sedimentary rock formations occur in three areas: the Mogilno-Lodz Basin, the Szczecin Basin and the Upper Silesian Block (Wójcicki et al., 2013). Potential HDR energy reservoirs are deeply deposited Lower and Middle Triassic, Lower Permian or Carboniferous formations (Sowiżdżał et al., 2013, 2022).

Since HDR/ EGS installations require a slow, conductive energy supply to the rocks of the production zone, the highest possible temperature, high thermal conductivity of the rocks and a uniform and balanced heat flow are desirable Therefore, from the point of view of modeling the future HDR/EGS systems, it is important to enrich the database of petrophysical parameters of rocks, especially their thermal parameters.

Thermal parameters are essential data in, among others, locating geothermal systems (Abdulagatova et al., 2009; Busby, 2016; Luo et al., 2016; Sowiżdżał and Kaczmarczyk, 2016; Zhang et al., 2019; Ma et al., 2020; Li et al., 2022) and geothermal modeling (Di Sipio et al., 2013). Thermal conductivity and diffusivity are important thermophysical properties of rocks, necessary to determine heat flow, assess the deep thermal regime and reconstruct the thermal history of sedimentation in the basins (Liu et al., 2011; Clauser and Huenges, 2013; Jeanloz and Stone, 2013).

Despite a lot of data of thermal parameters of igneous and metamorphic rocks, little attention has been paid to sedimentary rocks and heat flow in sedimentary basins in terms of the development of Enhanced Geothermal Systems (Deming, 1994; Mottaghy et al., 2008; Schön, 2015; Miranda et al., 2017; Miao and Zhou, 2018; Jiang et al., 2021). Geothermal studies of sedimentary rocks are mostly related to the search for hydrocarbons, thermal conductivity, burial depth and stratigraphic age (Wang et al., 2016). The thermal evolution of the source rocks and the resulting thermal maturity depend on the lithology of the sedimentation basin and the initial thermal conductivity of the rocks (Liu et al., 2011). In the case of sedimentary rocks, especially shale, which tend to be highly anisotropic, the direction in which the thermal conductivity is measured is also an important information (Labus and Labus, 2018). To estimate the Earth's heat flow, the appropriate thermal conductivity is that perpendicular to the bedding (Deming, 1994).

The aim of this research was determining the basic thermal parameters of rocks, i.e., effusivity, thermal conductivity and diffusivity, basing on tests of samples taken from boreholes, representing selected geothermal structures in Poland, representative of Central Europe, which are potential targets for EGS development.

2. Thermal parameters

Thermal conductivity (λ or k), is the heat (Q) transferred as a result of a unit temperature gradient under steady state conditions, through a unit area of a material layer of unit thickness under steady state conditions.

Another property, thermal effusivity (e is also known as thermal responsivity), required in the analysis of time-dependent conditions, reflects the ability of a material to exchange heat with its surroundings to store or dissipate heat. Thermal effusivity measures how well a material can exchange heat with any substance with which it comes into contact.

The values of thermal conductivity and effusivity allow the calculation of thermal diffusivity (α is also known as temperature compensation coefficient), a property that describes how quickly a material reacts to a change in temperature. It is a measure of the temperature change in a unitary volume of a material, caused by heat flowing per unit time through an object with a unit area and unit thickness, with a unit temperature difference between its surfaces.

Since diffusivity takes into account how much energy is absorbed when heating a material with a given temperature gradient, it tells more about what happens under transient heat flow conditions than about conductivity itself. Thus, thermal diffusivity describes how quickly a material initially exposed to transient heat conduction enters a steady-state heat flow state. This means that the temperature change over time is equal to the product of the thermal gradient of a given material and its diffusivity. To sum up: it is thermal diffusivity that determines the rate of heat conduction; materials with high thermal conductivity (k) and low heat capacity (possibly with low specific heat and density) are characterized by high diffusivity.

Thermal properties are related to the mineral composition, compaction (and consequently porosity) and anisotropy of the rock. Other important factors in rock formation are the volume ratios between the solid, liquid and gas phases and the moisture content. Thermal conductivity depends in complex ways on the composition and distribution of minerals in the rock matrix and fluids in the pore space (Chekhonin et al., 2012; Kirk and Williamson, 2012). It is commonly assumed that the thermal conductivity of rocks decreases with increasing temperature and increases with increasing pressure, and the effects of temperature and pressure oppose each other (Abdulagatova et al., 2009; Clauser and Huenges, 2013). Hence, in some studies these effects are negligible; however, it should be noted that it is necessary to take into account the water saturation in order to correct the thermal conductivity in situ. Laboratory measurements of the thermal conductivity of rocks obviously give different values than those found in the rock mass, especially at great depths. This is due to different temperature and pressure conditions. The changes in thermal properties are caused by the opening of microscopic cracks and fissures in rock samples brought from high pressure deep underground to atmospheric pressure at the surface (Walsh and Decker, 1966).

The thermal conductivity of rocks is usually in the range 0.4-7.0 W/(m·K). Low values are characteristic for dry, unconsolidated sedimentary rocks, such as gravel and sand. Higher values of thermal conductivity occur for most sedimentary and metamorphic rocks, while very high values are typical for felzitic igneous rocks. The best conductors of heat are rocks with a high quartz content (e.g., quartzite, sandstone), as well as rocks saturated with water (Schön, 2015). Blackwell and Steele (1989) provide the values of thermal conductivity for sandstones in the range of 2.50-4.20 W/(m·K), for shales: 1.05-1.45 W/(m·K), and for clay and silt: 0.8-1.25 W/(m·K).

When analyzing the influence of mineralogical composition on thermal properties, quartz content is considered to be the first-order factor, because it is characterized by high values of thermal conductivity: 6-7 W/(m·K). In the case of sedimentary rocks, porosity is also an important factor. When the pores are filled with air, which has a low thermal conductivity (0.026 W/(m·K)), the high porosity obviously reduces the thermal conductivity of the rock. When air is replaced with water (or brine) under water-saturated conditions, the thermal conductivity of the rock is higher. In addition to porosity, the origin of the sediment is also considered to be the factor controlling the thermal conductivity of sedimentary rocks (Clauser and Huenges, 2013).

3. Material and methods

3.1 Tested material

There were used 132 rock samples for the study, in the form of cores of 1.5-inch diameter, drilled from the borehole material, with aligned faces, representing the lithological types and geologic provinces presented in Table 1.

In relations to the stratigraphic position and the geological unit (Table 1, Fig. 1), the samples can be classified into 5 groups, as follows:

1) Middle Cambrian fine grained quartz sandstone from Leba Elevation, which is perspective zone for unconventional hydrocarbon resources (borehole 17).
2) Carboniferous fine-grained sandstones and siltstones from Lublin Synclinorium and Podlasie-Lublin Elevation (boreholes 11-16).
3) Permian (Rotliegend) medium-grained sandstones from Fore-Sudetic Monocline, which are potential for tight gas accumulation (boreholes 9-10).
4) Permian (Main Dolomite, Zechstein) carbonate rocks from Fore-Sudetic Monocline, which represent oil-prone source rocks (boreholes 5-8).
5) Upper Triassic and Middle Jurassic fine-grained sandstones and siltstones from Warszawa Synclinorium (boreholes 1-4).

As it can be noticed from the data included in the Table 1, the temperature measured in the boreholes at the given depths is differentiated. The formations recognized up to a depth of about 3,800 m within the Fore-Sudetic Monocline, and up to about 3,000 m in the Szczecin Synclinorium and the Leba Elevation are the high-temperature structures (100-135 °C).

Table 1. Summary of data on the analyzed samples.

No.	Borehole	Depth interval (m)	Temperature (°C)	Samples	Stratigraphy	Lithology
			Warszawa Synclinorium			
1	K-1	2,023.6-1,132.3	35-65	6		Fine-grained sandstone, (siltstone)
2	B-GN3	2,453.1-2,009.6	60-70	7	Middle Jurassic	Fine-grained sandstone
3	Ż-IG3	2,536.8-2,006.3	60-70	7		Sandstone, siltstone
4	R-2	2,165.5-968.4	30-60	10	Upper Triassic	Fine-grained sandstone
			Fore-Sudetic Monocline			
5	Ba-7	3,137.0-3,124.0	130-135	26		
6	B-1	3,132.7-3,132.6	130-135	2	Zechstein	Dolomite, dolomitic limestone
7	B-7	3,136.9-3,136.0	130-135	6		
8	B-5	3,139.8-3,139.7	130-135	9		
9	P-2	3,805.7-3,758.7	110-130	5	Rotliegend	Medium grained sandstone
10	P-1	3,813.7-3,789.2	110-130	10		
			Lublin Synclinorium			
11	U IG1	944.9	35	1		Siltstone
12	A-1	1,265.9-1,219.8	35-45	1		Fine-grained sandstone, (siltstone)
13	L IG2	1,435.7-1,064.3	40-50	10	Carboniferous	Fine-grained sandstone
14	B IG1	1,488.9-1,309.1	45-50	3		Siltstone
15	D-10	2,338.9-2,302.9	80-90	2		Fine-grained sandstone
			Podlasie-Lublin Elevation			
16	K IG2	1375.9-1164.8	45-50	5	Carboniferous	Fine-grained sandstone, (siltstone)
			Leba Elevation			
17	O-3	3,023.1-2,963.0	95-105	19	Middle Cambrian	Quartz fine-grained (sandstone)

Fig. 1. The position of boreholes within the geologic provinces of Poland. Numbers of the boreholes according to Table 1.

Warszawa Synclinorium and Lublin Synclinorium formations form the depth of 2,000-2,500 m can be recognized as medium-temperature structures (60-90 °C). Some samples, from depths from about 1,000 to 1,500 m, represent low temperature structures (with temperatures below 60 °C), such as Lublin Synclinorium and Podlasie-Lublin Elevation. The classification of geothermal resources, basing on the temperature, was implemented after Muffler and Cataldi (1978) and Górecki (2006).

3.2 Thermal measurements

The thermal conductivity of the samples was measured with the advanced C-Therm TCi thermal analyzer (New Brunswick, Canada). A schematic diagram of the measurement system is shown in Fig. 2. It consists of a single-sided interfacial heat reflection sensor, an optional sample container with a protective ring, a control unit and a data acquisition unit. Prepared, dry samples, coated with a contact material (Wakefield 120), were placed on the sensor and loaded with a weight to stabilize the contact. The TCi uses a modified tr-

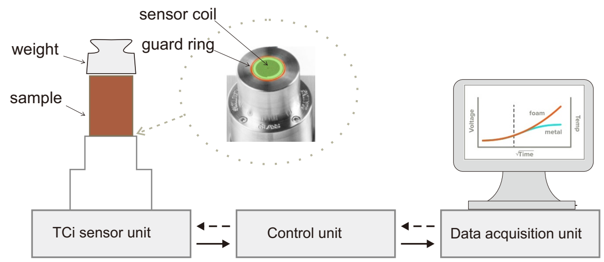

Fig. 2. Schematic diagram of the test stand for thermal conductivity measurement.

ansient plane source to measure the thermal conductivity of the material. A current of known voltage is applied to the spiral heating element of the sensor to deliver a small amount of heat to the sample is induced by the temperature rise at the interface between the sensor and the sample, the thermal properties of the sample can be determined. With a known heat flux through the sample and the temperature gradient, the thermal conductivity can be calculated according to the Fourier's law:

$$q=-k\frac{\mathrm{d}T}{\mathrm{d}x} \tag{1}$$

where q is heat flux density, $\mathrm{W/m^2}$; $\mathrm{d}T/\mathrm{d}x$ denotes temperature gradient, K/m; k is thermal conductivity coefficient, W/(m·K).

Other derivative values are determined indirectly, based on the results of thermal conductivity and effusivity tests, using the C-Therm TCi software. When testing at high temperatures or when using porous or absorbent materials, the use of traditional contact media (water or glycol) should be avoided as these may be absorbed by the sample material and affect the measurement. For this reason, due to the water absorption of the tested rocks, Wakefield 120 thermal grease was used as a substitute contact medium.

3.3 Petrophysical parameters

3.3.1 Porosity and permeability

The porosity coefficient is the basic indicator of the storage volume of a porous layer. It is defined as the ratio of the pore volume in a given sample to the total sample volume.

The methods of measuring the porosity coefficient do not take into account the morphology of the pore space. The parameterization of the pore space is achieved by interpreting capillary pressure curves. The values presented in the paper were obtained by the mercury injection porosimeter.

The porosimetric tests, regardless of the technical solutions, are based on a cylindrical model of the pore space, in which the pore space is simulated as a bundle of cylindrical capillaries transporting reservoir fluids. The distribution of the equivalent pores' diameters and their distribution in the tested pore space are obtained from the Washburn's equation:

$$d=\frac{\tau\cos\varphi}{4P} \tag{2}$$

where d stands for pore diameter, m; P is implemented pressure, Pa; φ is a contact angle between the rock and the fluid (wetting angle) (deg), τ denotes surface tension, N/m.

Knowing the mass of the sample and determining its external volume and the volume of the rock skeleton during porosimetric measurement, the obtained results are calculated from the Washburn's Eq. (2), thus obtaining the distribution of pore diameters in a given sample, as well as partial volumes as dynamic porosity of the sample, its skeletal density and bulk density.

The AutoPore IV mercury porosimeter used in the study allows to obtain two cumulative curves plotted for the intrusion and extrusion of mercury. Porosimetric measurements allow the calculation of the following values:

(1) Porosity (p), which is calculated from the porosimeter measurement. It differs from open porosity because the volume of non-wetting fluid that has migrated into the sample is taken into account. This volume does not include all submicropores that are too small in diameter to allow mercury to penetrate. Thus, the porosity value calculated from the porosimeter is smaller than the open porosity, and the difference is a measure of the amount of irreducible water in the sample. The measurement may be disturbed by the so-called "edge effect", which results from the unevenness of the surface of the tested sample and, as a result, causes an apparent increase in the porosity calculated from the porosimeter. This effect is significant for low porosity samples.

(2) Pore diameter, this is a standard value for assessing the quality of reservoir rocks. Average pore diameter (D_{ave}) is calculated as a weighted average, with the weight of the pore number rather than the percentage of pore space.

(3) Specific surface area (S_A), the total pore area per unit volume of the tested rock (it is a measure of the flow resistance in the porous material).

(4) Threshold diameter, in mathematical sense, it is the inflection point of the cumulative curve that represents a certain pressure (or diameter) value during porosity measurements. When it is exceeded, mercury saturation begins to increase very quickly with slight changes in pressure. The higher the value of the threshold diameter, the better the filtration properties of the tested rock. After a sharp increase in saturation, with a decrease in pore diameters, the cumulative curve tends asymptotically to the value of maximum saturation.

The results of the mercury injection porosimeter analyzes were used to calculate permeability using the Katz-Thompson and Swanson percolation model (Katz and Thompson, 1987; Swanson, 2007) and the Poiseuille model (Purcell, 1949).

3.3.2 Density

Density was measured with use of a helium pycnometer AccuPyc 1330. This device uses the excellent ability of helium to penetrate even the smallest submicropores. Then, the exact value of the skeleton density in the measurement is obtained. The procedure is as follows: the test sample is weighed and then placed in a calibrated chamber into which a specified amount of helium is injected. The skeleton volume of the test sample, and then the skeleton density, are calculated from the ideal gas equation. The same samples are then placed in the porosimeter. In porosimetric measurements, the bulk density of the test sample is obtained. After calculating the volume of the rock skeleton of the sample and its external volume, the open porosity coefficien can be calculated by:

$$p=\frac{V_b-V_{sk}}{V_b} \tag{3}$$

where p is an open porosity coefficient; V_b is external volume, m^3; V_{sk} is volume of the rock skeleton, m^3.

3.4 Calculation of energy resources

To calculate the total unit accessible resources at a given depth (E_T, J/m^3) (energy contained in a unit volume (1 m^3) of rock), referred to mean annual temperature (T_{ref}) (Muffler and Cataldi (1978)):

$$E_R=\rho_h c_h\left(T_h-T_{ref}\right) \tag{4}$$

where ρ_h stands for rock density at a given depth, kg/m^3; c_h is specific heat of rocks at a given depth, J/(kg·K); T_h is reservoir temperature at a given depth, °C; T_{ref} denotes reference temperature, °C (assumed as 9 °C after Rojek and Usowicz (2018)).

The static energy resources of geothermal reservoirs per unit volume (1 m^3) of rock (E_{WR}), represent the amount of accumulated heat in the free water contained in the pore and fracture space (E_W), and in the rock matrix (E_R) of a given layer or aquifer, therefore they can be calculated by:

$$E_{WR}=E_W+E_R \tag{5}$$

$$E_{WR}=\left[\left(1-p_e\right)\rho_s c_s+p_e\rho_w c_w\right]\left(T_h-T_{ref}\right) \tag{6}$$

where p_e is effective porosity; ρ_s and ρ_w mean density of rock matrix and water, respectively, kg/m^3; c_s and c_w mean specific heat of rock matrix and water, respectively, J/(kg·K).

Due to the relatively poor reservoir parameters of rocks, and high total dissolved solids in geothermal water in Poland, for maintenance of the hydrogeological regime, it seems necessary to use geothermal doublet exploitation systems. The part of the geological resources extracted from a given reservoir is determined by the recovery factor R_0:

$$R_0=\frac{A_s}{A_c}\frac{T_h-T_c}{T_h-T_{ref}}=0.33\frac{T_h-T_c}{T_h-T_{ref}} \tag{7}$$

where A_s is the area of the reservoir cooled by the doublet system, m^2; A_c is the total area of the reservoir influenced by the doublet system, m^2; T_c denotes the temperature of the cooled waters reinjected to the reservoir, °C (assumed to be 25 °C).

In order to allow comparisons with the geothermal resources previously calculated for the Polish conditions (Górecki, 2006), the ratio of the cooled area to the total doublet area of interaction was adopted, as empirically determined constant value of 0.33, according to long-term experiences of geothermal installations within the Paris Basin, France.

Static, recoverable resources per unit volume (E_{Rec}) are calculated by:

$$E_{Rec}=R_0E_{WR} \tag{8}$$

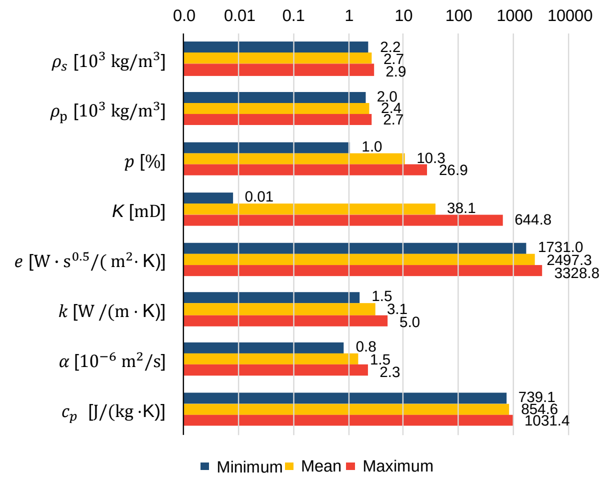

Fig. 3. Descriptive statistics of selected parameters of the analyzed rocks ($N = 132$).

4. Results

4.1 Petrophysical and thermal parametrs

The values of petrophysical and thermal parameters of the analyzed samples are within fairly wide ranges (Fig. 3). The heat capacity coefficient (c_p) is a parameter that depends on the rock density.

Taking into account all the analyzed samples, the following correlations between the tested parameters can be noticed-Table 2: the bulk heat capacity coefficient (c_p) is negatively correlated with density and positively with the content of pores sized above 1 μm, the value of the threshold diameter and porosity. The latter correlation is due to the fact that during the measurements the pores of the rocks were filled with air, which has a relatively high specific heat compared to quartz or dolomite, the main components of the grain skeleton. Similar but moderate correlations with density and porosity are visible also for effusivity (e), thermal conductivity (k) and diffusivity (α), which in turn, are related to each other. In order to obtain the more detailed insight into the nature of the parameters shown in Fig. 3, they were analyzed by the following lithological groups: siltstones, fine-grained sandstones, medium-grained sandstones and carbonate rocks. After discarding outliers, the following observations become visible:

- The skeletal density (ρ_s) of carbonate rocks (mainly dolomites) is the highest, and ranges from about 2.64 to 2.90×10^3 kg/m^3. For the other lithological types, it ranges from 2.21 to 2.74×10^3 kg/m^3.
- The porosimeter (bulk) density (ρ_p) of carbonate rocks is again the highest, and ranges from about 2.30 to 2.65×10^3 kg/m^3. The lowest bulk density is for medium-grained sandstones-from 1.98 to 2.38×10^3 kg/m^3.
- Porosity (p) is the least diversified in the case of siltstones from 1.22% to 5,76% and medium-grained sandstones from 8.49% to 15.18%. However, it should be noted that both these groups include relatively few samples (10 and 21 respectively).

Table 2. Pearson Correlation Coefficients for selected parameters of the analyzed rocks.

Parameter	ρ_s	ρ_p	p	e	k	α	c_p	D_{ave}	S_A	D_{th}	Micropores (> 1µm)
ρ_s	1.00	0.40	0.20	0.10	0.10	0.10	-0.35	0.13	-0.37	-0.27	-0.24
ρ_p	0.40	1.00	-0.82	0.37	0.38	0.37	-0.81	-0.41	-0.16	-0.54	-0.57
p	0.20	-0.82	1.00	-0.34	-0.35	-0.33	0.65	0.53	-0.07	0.40	0.47
e	0.10	0.37	-0.34	1.00	1.00	1.00	0.23	0.01	-0.37	-0.09	-0.17
k	0.10	0.38	-0.35	1.00	1.00	1.00	0.22	0.01	-0.37	-0.10	-0.17
α	0.10	0.37	-0.33	1.00	1.00	1.00	0.23	0.01	-0.37	-0.09	-0.17
c_p	-0.35	-0.81	0.65	0.23	0.22	0.23	1.00	0.45	-0.08	0.51	0.52
D_{ave}	0.13	-0.41	0.53	0.01	0.01	0.01	0.45	1.00	-0.55	0.32	0.68
S_A	-0.37	-0.16	-0.07	-0.37	-0.37	-0.37	-0.08	-0.55	1.00	-0.04	-0.36
D_{th}	-0.27	-0.54	0.40	-0.09	-0.10	-0.09	0.51	0.32	-0.04	1.00	0.54
Micropores (> 1µm)	-0.24	-0.57	0.47	-0.17	-0.17	-0.17	0.52	0.68	-0.36	0.54	1.00

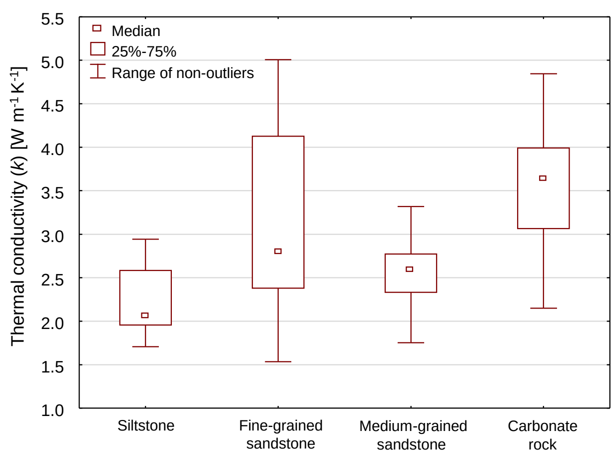

Fig. 4. Variability of thermal conductivity in the lithological groups of the studied rocks.

- A clear difference in thermal parameters between lithological groups concerns thermal conductivity (k) and diffusivity (α), which are correlated with each other. Siltstones and medium-grained sandstones are characterized by low thermal conductivity (1.71 to 2.94 W/(m·K) and 1.75-3.32 W/(m·K) respectively). Significantly higher values of thermal conductivity represent carbonate rocks (dolomites and dolomitic limestones)-up to 5.06 W/(m·K), with median of 3.64 W/(m·K) (Fig. 4).
- Thermal conductivity values for the particular lithological groups of samples fall within the ranges given in the literature by other authors, e.g., Liu et al. (2011), Clauser and Huenges (2013), Eppelbaum et al. (2014), Jiang et al. (2021).
- Bulk heat capacity coefficient (c_p) is for siltstones from 764 to 896 J/(kg·K), fine-grained sandstones 765-1,002 J/(kg·K), medium-grained sandstones 807-992 J/(kg·K), and for carbonates 739-1,031 J/(kg·K).

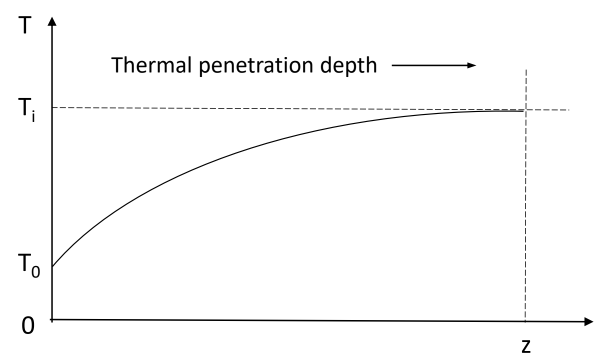

Fig. 5. Heat conduction in a semi-infinite domain.

- Effusivity (e) for siltstones ranges from 1,804 to 2,437 W·s$^{0.5}$/(m^2 · K), fine-grained sandstones 1,731-3,329 W·s$^{0.5}$/(m^2 · K), medium-grained sandstones 1,774-2,881 W·s$^{0.5}$/(m^2 · K), and for carbonates 2,050-3,264 W·s$^{0.5}$/(m^2 · K).
- Diffusivity (α) for siltstones ranges from 0.859-1.46×10^{-6} m^2/s, fine-grained sandstones 0.75-2.26×10^{-6} m^2/s, medium-grained sandstones 0.28-1.86×10^{-6} m^2/s, and for carbonates 1.10-2.20×10^{-6} m^2/s.

4.2 Evolution of formation temperature and depth of thermal penetration

In order to investigate the impact of the examined thermal parameters on the behavior of rocks during the possible exploitation of geothermal resources, analytical calculations were performed, which allowed to determine the evolution of temperature and the depth of thermal penetration inside the formations during their cooling down during operation.

The formation model has been simplified to a 1-D half-domain, which is infinite in one coordinate direction ($z \to \infty$) (Fig. 5).

Table 3. Descriptive statistics of selected parameters of the analyzed rocks in geologic provinces ($N = 132$).

Group	Geologic province		p	K	k	α	e	C
I	Leba Elevation	mean	3.813	0.046	4.184	1.951	2984.3	839.275
		min	1.632	0.008	2.645	1.328	2295.344	766.621
		max	6.18	0.284	5.006	2.262	3328.789	890.557
		SD	1.542	0.078	0.643	0.25	277.955	32.8155
II	Lublin Synclinorium and Podlasie-Lublin Elevation	mean	8.812	62.062	2.37	1.195	2126.69	832.785
		min	1.03	0.048	1.534	0.785	1730.98	765.306
		max	20.51	644.762	3.545	1.707	2712.951	938.511
		SD	5.608	147.646	0.493	0.226	252.498	49.9493
III	Fore-Sudetic Monocline	mean	11.691	0.563	2.541	1.278	2242.664	849.254
		min	8.492	0.104	1.754	0.901	1847.664	806.657
		max	15.18	0.868	2.93	1.453	2430.979	878.826
		SD	2.032	0.189	0.315	0.147	155.695	17.5794
IV	Fore-Sudetic Monocline	mean	11.733	4.435	3.53	1.696	2703.016	840.347
		min	1.65	0.037	2.149	1.098	2050.409	739.06
		max	22.75	31.389	4.845	2.203	3264.192	1031.437
		SD	4.345	7.009	0.686	0.287	308.736	50.6409
V	Warszawa Synclinorium	mean	12.975	76.028	2.692	1.336	2330.317	904.461
		min	2.85	0.13	1.707	0.877	1822.909	763.407
		max	26.89	378.185	4.569	2.101	3152.139	1002.359
		SD	7.801	98.91	0.686	0.293	298.359	66.4359

Notes: C is the heat capacity, J/(kg·K).

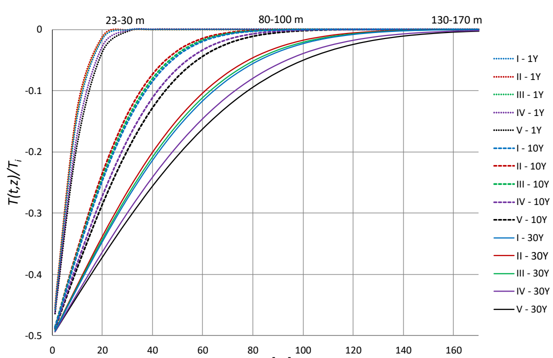

Fig. 6. Evolution of the relative temperature ($T(t,z)/T_i$) with depth (z). Explanations: roman numbers-formation groups I-V (according to Table 3); time: 1 year-1Y, 10 years-10Y, 30 years-30Y.

The parameters described above are also presented in Table 3, which takes into account the geological unit, according to the previously proposed division (Fig. 1).

The temperature loss at a distance x from the boundary, after a drop from the initial temperature at the surface, can be calculated according to the analytical solution based on heat conduction equation:

$$T(t,z) = T_i + (T_0 - T_i) \cdot \operatorname{erfc}(\frac{z}{\sqrt{4\alpha t}}) \tag{9}$$

where $T(t,z)$ stands for temperature at a time-t, and distance-z, from the boundary, °C; T_i is an initial temperature, °C; T_0 stands for temperature at the surface at time t = 0, °C; t means time, s; z is a distance from the domain border, m; α is thermal diffusivity, m^2/s; erfc means complementary error function.

Fig. 6 shows the evolution of the relative temperature ($T(t,z)/T_i$) with depth, from the surface of the analyzed half-space (the "minus" sign stands for cooling).

The resulting curves are grouped in three clusters corresponding to the time of 1, 10 and 30 years of cooling the surface of the thermal system, assuming that the temperature on the surface is half the initial temperature of the massif ($T_0 = 0.5T_i$). In each of the clusters there are differences in the course of relative temperature curves, the largest range of changes in relative temperature (penetration depth) is visible for the formation with the highest mean diffusivity value-Formation I-Leba Elevation, and the smallest in Formation II-Lublin Synclinorium and Podlasie-Lublin Elevation (Table 3), where after 1 year of cooling it is respectively about 30

Table 4. Temperature drops and thermal penetration depths for 1, 10 and 30 years of simulated heat extraction.

Group	Temperature drop (°C)			Penetration depth (m)		
	1Y	10Y	30Y	1Y	10Y	30Y
I	3	10	18	22	84	145
II	4	14	25	19	61	118
III	4	14	24	20	70	130
IV	3	73	140	21	73	140
V	4	13	23	21	65	122

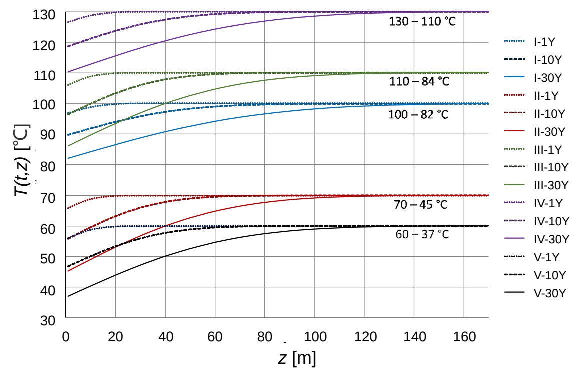

Fig. 7. Evolution of temperature ($T(t,z)$) with depth (z). Explanations: roman numbers-formation groups I-V (according to Table 3); time: 1 year-1Y, 10 years-10Y, 30 years-30Y.

and 23 m, and after 30 years-170 and 130 m.

For the described 1-D half-domain, the temperature drop ($T(t,z)$) at a distance (z) from the boundary, due to an assigned heat flux (q), cooling at the surface, can be calculated according to the analytical formulae:

$$\frac{T(t,z)-T_0}{T_i-T_0} = \mathrm{erf}\left(\frac{z}{\sqrt{4\alpha t}}\right) \tag{10}$$

$$q = \frac{k(T_0-T_i)}{\sqrt{\pi\alpha t}} \tag{11}$$

From which the following solution can be derived:

$$T(t,z) = T_i + \frac{q\sqrt{\pi\alpha t}}{k}\mathrm{erfc}\left(\frac{z}{\sqrt{4\alpha t}}\right) \tag{12}$$

where erf is error function.

Calculations for the solution of heat conduction in a semi-infinite body under the specified heat flux were carried out for the values α-mean diffusivity and k-thermal conductivity for a certain formation (Table 3) and Ti-means temperature for a certain formation. They made it possible to compare the behavior of individual formations in identical conditions of heat extraction, assuming that the heat flux $q=-1$ W/m^2. For such a value, after 30 years of simulated heat production, for the formation V (Warszawa Synclinorium), with the lowest initial temperature, the final temperature value was not lower than 35 °C. Temperature drops and thermal penetration depths resulting from heat extraction at the domain boundary for individual formations are presented in Table 4 and visualized in the Fig. 7.

As in the case of calculations made on the basis of the temperature drop assumption, also here the greatest range of temperature changes (penetration depth) is visible for the formations with the highest mean diffusivity and thermal conductivity-Formation I (Leba Elevation), and the smallest in Formation II (Lublin Synclinorium and Podlasie-Lublin Elevation), where after 1 year of cooling it is about 22 and 19 m, respectively, and after 30 years-145 and 118 m.

The temperature drop is the lowest for: I-Leba Elevation and IV-Fore-Sudetic Monocline which are the formations with the highest thermal conductivity and diffusivity values. It is noteworthy that in the Formation III-Fore-Sudetic Monocline, a relatively significant decrease in temperature was calculated, related to its low parameters α and k. Due to the high initial temperature of this formation, however, this is not a phenomenon that would deplete the reservoir resources, negatively affecting the possibility of continuing exploitation even in the long term (for 30 years of simulated heat extraction the temperature levels at 110 °C). The situation is different in the case of Formation II-Lublin Synclinorium and Podlasie-Lublin Elevation, and Formation V-Warszawa Synclinorium, where the temperatures after simulated 30 years will be only 45 and 37 °C, respectively.

4.3 Resources

The total unit accessible resources at a given depth-E_T (energy contained in a unit volume (1 m^3) of rock) were calculated basing on the formulas presented in chapter 3.4. The highest resources are found in the high temperature collectors, respectively, in the Zechstein formations, in the Rotliegend and the Middle Cambrian. Despite the relatively high porosity of the Middle Jurassic and Carboniferous rocks, their resources are more than twice and three times smaller, respectively. The resources per unit rock volume, calculated based on the samples representing the analyzed geologic provinces, are shown in the Table 5.

5. Discussion

From the point of view of the suitability of reservoir rocks for EGS systems, it is important to find rocks with the lowest porosity and the highest thermal conductivity. The graph in Fig. 8 presents the relationship of these two parameters. As it is visible, the correlation between them is rather weak, but from the point of view of suitability for use in EGS, one can notice that rocks with relatively low porosity and high thermal conductivity (red square 1 field in Fig. 8) belong to a large group of fine-grained sandstones. Moreover, it turns out, that if taking into account the classification presented in Table 3, the fine-grained sandstones with the best ratio of porosity vs. thermal conductivity belong to group I (Middle Cambrian fine grained quartz sandstones from Leba Elevation) and group V (Upper Triassic and Middle Jurassic fine-grained sandstones from Warszawa Synclinorium). However, it should be remembered that the last group (V) belongs to medium-temperature structures (60-90 °C).

Table 5. Resources per unit rock volume in the analyzed geologic provinces.

Group	Depth (m)	Temperature (°C)	Lithology	Porosity/Permeability ratio (Fig.9)	Resources (MJ/m^3)		
					E_T	E_{WR}	E_{Rec}
I	3,023.1-2,963.0	95-105	Fine-grained quartz sandstone	EGS petrothermal	205.0	211.0	57.9
II	2,338.9-944.5	35-90	Fine-grained sandstones and siltstones	All	68.0	73.8	13.2
III	3,813.7-37,58.7	110-130	Medium-grained sandstones	EGS hydrothermal	240.0	271.0	77.7
IV	3,139.8-3,124.0	130-135	Carbonate rocks	EGS hydrothermal	262.0	293.0	84.4
V	2,536.8-968.4	35-70	Fine-grained sandstones and siltstones	All	89.4	99.6	21.1

Notes: E_T is total accessible resources, E_{WR} is static resources.

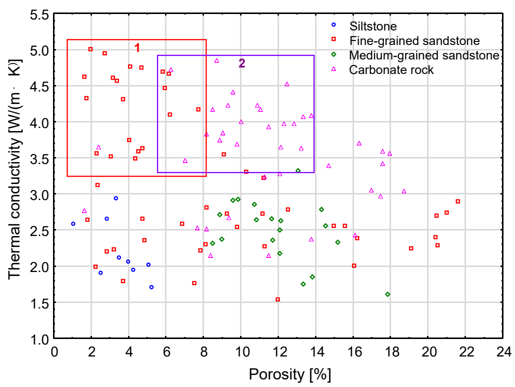

Fig. 8. Relationship of thermal conductivity to porosity with respect to lithological types of rocks.

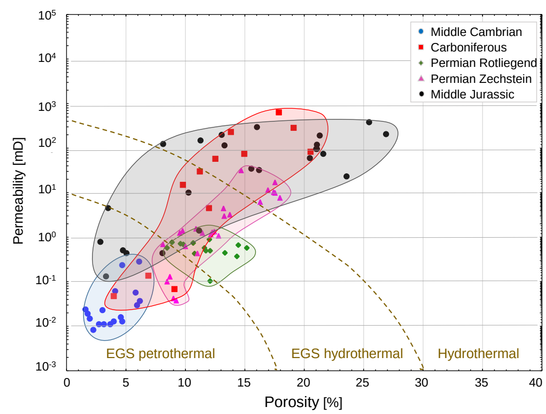

Fig. 9. Correlation between permeability and porosity with respect to distinguished lithostratigraphical groups and the correspondence to EGS and hydrothermal settings (after Moeck (2014) and Kudrewicz (2022)).

On the other hand, as can be seen from the example of fine-grained sandstones, which are quite a large group of the rocks studied, the values of the parameters under consideration do not directly depend on the lithology. Then, when determining the petrophysical and thermal parameters of the rock, first of all, the geological situation of a given formation should be taken into account.

The next group distinguished in Fig. 8, of a good porosity-to-conductivity ratio (purple rectangle 2 field in Fig. 8), represents Permian (Main Dolomite, Zechstein) carbonate rocks from Fore-Sudetic Monocline. As it was presented in Table 1, this structure is also a high-temperature one, hence it is prospective when addressing the development of EGS systems.

The important parameter in evaluating geothermal play systems is the ratio of porosity to permeability of rocks. Usually, both the permeability and the porosity decrease with increasing depth of the considered formation, which results from high static stresses and an advanced degree of diagenesis. Hence, the depth of the geothermal system taken into account might be an important factor for successful long-term reservoir production (Moeck, 2014). The graph presented in Fig. 9 illustrates the porosity-versus-permeability diagram with regard to reservoir rock type (Moeck, 2014). A similar reservoir classification scheme has been developed by Salley (2000) for hydrocarbon resources.

On the basis of the above diagram (Fig. 9), it can be seen that silicoclastic rocks of the Middle Cambrian are characterized by extremely low values of porosity and permeability, which fully classifies this group as possibly favorable for EGS petrothermal development. The samples representing the Permian Rotliegend medium-grained sandstones and Permian Zechstein also rank in the compact groups with relatively low porosity and permeability, indicating their suitability for use in EGS hydrothermal systems. Within the rocks representing the remaining groups distinguished in the diagram (Carboniferous and Middle Jurassic Fig. 9), there is a greater variation in the ratio of porosity to permeability, which makes the unequivocal classification difficult.

Thermal conductivity positively correlates with diffusivity. It can therefore be concluded that the higher the k value of a rock (the more energy can be extracted from the thermal source), the faster the absorbed energy is dissipated by it, and the gained energy is replenished from distant parts of the collector, due to high diffusivity, which is confirmed by the evolution of the relative temperature ($T(t,z)/T_i$) (Fig. 6), the

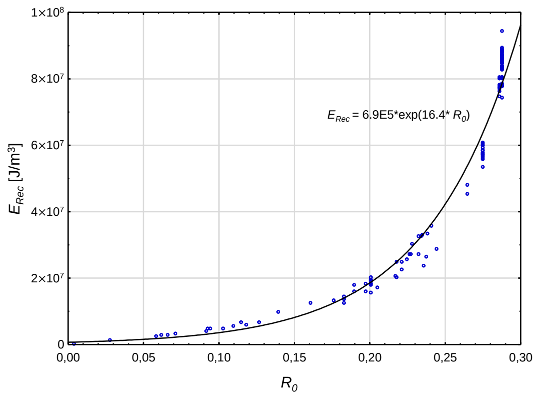

Fig. 10. Static, recoverable resources (E_{Rec}), vs. the recovery factor (R_0).

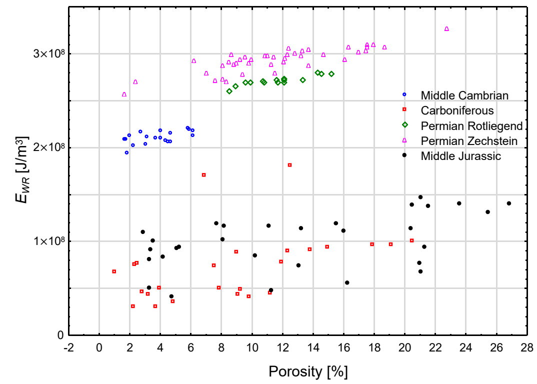

Fig. 11. Static resources (E_{WR}) vs. porosity.

penetration depth (Table 4), and temperature drop in the formations (Fig. 7). In this respect, quartz fine-grained sandstones from Leba Elevation and Zechstein dolomites a have the most favorable parameters, while the Carboniferous sandstones are the least suitable. Although a significant temperature drop was assessed for the Rotliegend sandstones of Fore-Sudetic Monocline, associated with relatively low diffusivity and thermal conductivity, due to the high initial temperature of this formation, the possibility of heat extraction will be realistic even in the long term.

Hydraulic fracturing is an efficient technology to develop thermal collector in EGS, formed in hot, dry, low-permeable rocks. The artificially created fracture network in the collector allows for the forced flow of the technological fluid in the loop between the production and injection wells. The fluid is heated in the collector, then pumped to the surface and, after cooling, injected back into the formation (Moska et al., 2021). In this context, the thermal parameters, such as thermal conductivity and thermal diffusivity, of rocks are of key importance to ensure efficient heat transfer between the formation and the working fluid. When a medium (cold working fluid) is injected in the underground, the implication would be that a good thermal diffuser (e.g., quartz-dominated rocks) approaches its thermal equilibrium faster than comparatively worse thermal diffusers, such as clay-rich or carbonate rocks (Fuchs et al., 2021). Referring to these findings, it should be stated that among the rocks analyzed by us, not only the quartz sandstones (Table 3-Group I), but also the dolomites (Table 3-Group IV) turn out to have favorable thermal properties.

Thermal conductivity reflects the ability of a material to conduct heat, while thermal diffusivity refers to the rate of transfer of heat of a material from its hot end (e.g., internal part of a geothermal collector) to the cold end (e.g., a fracture plane created in an engineered geothermal system-EGS in low-permeable HDR). Heat spreads faster through materials with high thermal diffusivities, which absorb or return heat to the external area faster, and therefore reach thermal equilibrium more quickly.

Thermal effusivity of a material has a significant influence on its heat release (Yang et al., 2016), and therefore the higher rock effusivities enable better heat deliverability rate, during the geothermal reservoir operation. Effusivity is not only indicative on heat exchange between two material bodies, and how much heat can be released or stored in dynamic processes, but it also influences stresses and thermal deformations during heat conduction in unsteady conditions and plays a key role in thermal fatigue and thermal shock, which should be taken into account in the appropriate selection of cements for well completion, and working fluid temperature and properties, as well as the injection rate, particularly in the initial period of operation of the EGS systems.

Thermal effusivity and diffusivity represent two competing phenomena: the first is related to the material's ability to absorb heat, the second-to the rate at which it reaches thermal equilibrium, namely to adapt to its surroundings. In other words, diffusivity is related to heat penetration and effusivity to surface heat transfer (Salazar, 2003; Dante, 2016). For the performance of geothermal systems, it is desirable that the effusivity, diffusivity, heat capacity and thermal conductivity of rocks are high. From this point of view, the Cambrian rocks belonging to Leba Elevation and Zechstein rocks from the Fore-Sudetic Monocline have again the most appropriate parameters, also taking into account the deposit temperatures. The rocks of Lublin Synclinorium and Podlasie-Lublin Elevation turn out to be the least suitable in this respect (Table 3).

The reservoir temperature has the greatest impact on the resources in each category. The exponential relationship between the recovery factor (R_0) and static, recoverable resources (E_{Rec}), shown in the Fig. 10, indicates a strong dependence of this parameter on the reservoir temperature (T_h). According to the Eq. (7), as the reservoir temperature T_h-(temperature at the top of the reservoir) increases, the significance of temperature of the cooled waters reinjected to the reservoir (T_c) and reference temperature (T_{ref}) decreases, and the R_0 value approaches asymptotically to the limit of 0.33. Resources are affected to a lesser extent by porosity (see Fig. 11), heat capacity and bulk density of rocks, while the rock matrix density is not clearly correlated with them.

6. Conclusions

(1)The conducted research allowed to obtain data on thermal parameters of sedimentary rocks which are rarely described in the literature. The selected rocks are representative of Central Europe as potential targets for EGS development.

(2) The fine-grained quartz sandstones from the Leba Elevation and Zechstein dolomites from the Fore-Sudetic Monocline, as rocks with the highest diffusivity, will approach thermal equilibrium faster than other tested rocks after injection of cold working fluid in EGS systems.

(3) From the point of view of EGS systems the best ratio of porosity to thermal conductivity is found in fine-grained quartz sandstones of Middle Cambrian from the Leba Elevation, and Permian carbonate rocks from the Fore-Sudetic Monocline.

(4) Low porosity and permeability values classify the Middle Cambrian silicoclastic rocks as potentially favorable for the development of petrothermal EGS, while the medium-grained Rotliegend sandstones, and Zechstein dolomites, with slightly higher values of these parameters, are more suitable for hydrothermal EGS.

(5) The tests of rocks from deep boreholes showed, that the Cambrian rocks of the Leba Elevation and Zechstein rocks of the Fore-Sudetic Monocline are characterized by the most suitable parameters from the point of view of obtaining geothermal energy from the Enhanced Geothermal Systems in Poland. Although Rotliegend sandstones of the Fore-Sudetic Monocline are characterized by relatively low diffusivity and thermal conductivity, due to the high initial temperature, this formation offers encouraging prospects for heat exploitation even in the long term.

Acknowledgements

This paper was partially funded as part of statutory work realized at the Silesian University of Technology.

Conflict of interest

The authors declare no competing interest.

References

Abdulagatova, Z., Abdulagatov, I. M., Emirov, V. N. Effect of temperature and pressure on the thermal conductivity of sandstone. International Journal of Rock Mechanics and Mining Sciences, 2009, 46(6): 1055-1071.

Blackwell, D. D., Steele, J. L. Heat flow and geothermal potential of Kansas. Kansas Geological Survey Bulletin, Department of Geological Sciences Southern Methodist University, Dallas, Texas, 1989, 226: 267-295.

Boden, D. R. Geologic Fundamentals of Geothermal Energy. Boca Raton, USA, CRC Press, 2017.

Brown, D. W., Duchane, D. V., Heineken, G., et al. The enormous potential of hot dry rock geothermal energy, in Mining the Earth's Heat: Hot Dry Rock Geothermal Energy, edited by D. W. Brown, G. Heiken, V. T. Hriscu, et al., Heidelberg, Springer Science & Business Media, Berlin, pp. 17-40, 2012.

Bujakowski, W., Barbacki, A., Miecznik, M., et al. A structural-thermal model of the Karkonosze Pluton (Sudetes Mountains, SW Poland) for hot dry rock (HDR) geothermal use. Archives of Mining Sciences, 2016, 61(4): 917-935.

Bujakowski, W., Bielec, B., Miecznik, M., et al. Reconstruction of geothermal boreholes in Poland. Geothermal Energy, 2020, 8: 10.

Busby, J. Thermal conductivity and diffusivity estimations for shallow geothermal systems. Quarterly Journal of Engineering Geology and Hydrogeology, 2016, 49(2): 138-146.

Chekhonin, E., Parshin, A., Pissarenko, D., et al. When rocks get hot: Thermal properties of reservoir rocks. Oilfield Review, 2012, 24(3): 20-37.

Clauser, C., Huenges, E. Rock thermal conductivity of rocks and minerals, in Physics and Phase Relations: A Handbook of Physical Constants, edited by T. J. Ahrens, American Geophysical Union, Washington, pp. 105-126, 2013.

Cui, G., Ren, S., Dou, B., et al. Geothermal energy exploitation from depleted high-temperature gas reservoirs by recycling CO_2: The superiority and existing problems. Geoscience Frontiers, 2021, 12(6): 101078.

Dante, R. C. Handbook of Friction Materials and their Applications. Amsterdam, Holland, Woodhead Publishing, 2016.

Deming, D. Estimation of the thermal conductivity anisotropy of rock with application to the determination of terrestrial heat flow. Journal of Geophysical Research, 1994, 99(B11): 22087-22091.

Di Sipio, E., Chiesa, S., Destro, E., et al. Rock thermal conductivity as key parameter for geothermal numerical models. Energy Procedia, 2013, 40: 87-94.

Eppelbaum, L., Kutasov, I., Pilichin, A. Applied Geothermics. Heidelberg, Berlin, Springer, 2014.

Fuchs, S., Forster, H. -J., Norden, B., et al. The thermal diffusivity of sedimentary rocks: Empirical validation of a physically based $\alpha-\phi$ relation. Journal of Geophysical Research: Solid Earth, 2021, 126(3): e2020JB020595.

Górecki, W. Atlas of geothermal resources in the Polish Lowlands-Paleozoic formations. Department of Fossil Fuels, Kraków, AGH-UST, 2006.

Górecki, W., Sowiżdżał, A., Hajto, M., et al. Atlases of geothermal waters and Energy resources in Poland. Environmental Earth Sciences, 2015, 74: 7487-7495.

Huenges, E., Ledru, P. Geothermal Energy Systems Exploration: Development and Utilization. Potsdam, Germany, Wiley-VCH, 2010.

Jeanloz, R., Stone, H. Enhanced geothermal systems. The MITRE Corporation, McLean, Virginia, Jason Program Office, 2013.

Jiang, X., Wu, C., Fang, X., et al. A new thermal conductivity estimation model for sandstone and mudstone based on their mineral composition. Pure and Applied Geophysics, 2021, 178: 3971-3986.

Katz, A. J., Thompson, A. H. Prediction of rock electrical conductivity from mercury injection measurements. Journal of Geophysical Research, 1987, 92(B1): 599-607.

Kepinska, B. Current geothermal activities and prospects in Poland-An overview. Geothermics, 2003, 32(4-6): 397-

407.

Kirk, S., Williamson, D. M. Structure and thermal properties of porous geological materials. AIP Conference Proceedings, 2012, 1426: 867.

Kudrewicz, R., Papiernik, B., Hajto, M., et al. Subsalt rotliegend sediments-A new challenge for geothermal systems in Poland. Energies, 2022, 15(3): 1166.

Labus, M., Labus, K. Thermal conductivity and diffusivity of fine-grained sedimentary rocks. Journal of Thermal Analysis and Calorimetry, 2018, 132: 1669-1676.

Li, H., Ji, K., Tao, Y., et al. Modelling a novel scheme of mining geothermal energy from hot dry rocks. Applied Sciences, 2022, 12(21): 11257.

Liu, S., Feng, C., Wang, L., et al. Measurement and analysis of thermal conductivity of rocks in the Tarim Basin, Northwest China. Acta Geologica Sinica, 2011, 85(3): 598-609.

Luo, J., Jia, J., Zhao, H., et al. Determination of the thermal conductivity of sandstones from laboratory to field scale. Environmental Earth Sciences, 2016, 75(16): 1158.

Ma, Y., Li, S., Zhang, L., et al. Numerical simulation on heat extraction performance of enhanced geothermal system under the different well layout. Energy Exploration and Exploitation, 2020, 38(1): 274-297.

Miao, S., Zhou, Y. Temperature dependence of thermal diffusivity and conductivity for sandstone and carbonate rocks. Journal of Thermal Analysis and Calorimetry, 2018, 131: 1647-1652.

Miranda, M. M., Rodrigues, N. V., Willis-Richards, J., et al. Assessment of deep geothermal energy potential in Northern and Central Portugal. European Geologist Journal, 2017, 43: 34-39.

Moeck, I. S. Catalog of geothermal play types based on geologic controls. Renewable and Sustainable Energy Reviews, 2014, 37: 867-882.

Moska, R., Labus, K., Kasza, P. Hydraulic fracturing in enhanced geothermal systems-field, tectonic and rock mechanics conditions-A review. Energies, 2021, 14(18): 5725.

Mottaghy, D., Vosteen, H. -D., Schellschmidt, R. Temperature dependence of the relationship of thermal diffusivity versus thermal conductivity for crystalline rocks. International Journal of Earth Sciences, 2008, 97: 435-442.

Muffler, P., Cataldi, R. Methods for regional assessment of geothermal resources. Geothermics, 1978, 7(2-4): 53-89.

Potter, R., Robinson, E., Smith, M. Method of extracting heat from dry geothermal reservoirs. US Patent No. 3786858, 1974.

Purcell, W. R. Capillary pressures-their measurement using mercury and the calculation of permeability therefrom. Journal of Petroleum Technology, 1949, 1(2): 39-48.

Rojek, E., Usowicz, B. Spatial variability of soil temperature in Poland. Acta Agrophysica, 2018, 25(3): 289-305.

Salazar, A. On thermal diffusivity. European Journal of Physics, 2003, 24(4): 351-358.

Saley, R. Applied Sedimentology, 2nd Ed. Burlington (MA), American, Academic Press, 2000.

Santos, L., Dahi Taleghani, A., Elsworth, D. Repurposing abandoned wells for geothermal energy: Current status and future prospects. Renewable Energy, 2022, 194: 1288-1302.

Schön, J. H. Physical Properties of Rocks: Fundamentals and Principles of Petrophysics (2nd edition). Development in Petroleum Science, 2015, 65: 2-497.

Sowiżdżał, A., Górecki, W., Hajto, M. Geological conditions of geothermal occurrences in Poland. Geological Quarterly, 2020, 64: 185-196.

Sowiżdżał, A., Kaczmarczyk, M. Analysis of thermal parameters of Triassic, Permian and Carboniferous sedimentary rocks in central Poland. Geological Journal, 2016, 51(1): 65-76.

Sowiżdżał, A., Machowski, G., Krzyżak, A., et al. Petrophysical evaluation of the Lower Permian formation as a potential reservoir for CO_2-EGS-Case study from NW Poland. Journal of Cleaner Production, 2022, 379(Part 2): 134768.

Sowiżdżał, A., Papiernik, B., Machowski, G., et al. Characterization of petrophysical parameters of the Lower Triassic deposits in a prospective location for Enhanced Geothermal System (central Poland). Geological Quarterly, 2013, 57(4): 729-744.

Swanson, B. F. A simple correlation between permeabilities and mercury capillary pressures. Journal of Petroleum Technology, 1981, 33(12): 2498-2504.

Tester, J. W. The Future of geothermal energy impact of enhanced geothermal systems (EGS) on the United States in the 21st century. Idaho National Laboratory, Idaho Falls, Massachusetts Institute of Technology, 2006.

Tomaszewska, B., Sowiżdżał, A., Chmielowska, A. Selected technical aspects of well construction for geothermal Energy utilization in Poland. Contemporary Trends in Geoscience: The Journal of Uniwersytet Slaski, 2018, 7(2): 188-199.

Walsh, J. B., Decker, E. R. Effect of pressure and saturating fluid on the thermal conductivity of compact rock. Journal of Geophysical Research, 1966, 17(12): 3053-3061.

Wang, A., Sun, Z., Liu, J., et al. Thermal conductivity and radioactive heat-producing element content determinations for rocks from Zhangzhou region, SE China, and their constraints on lithospheric thermal regime. Environmental Earth Sciences, 2016, 75: 1213.

Wójcicki, A., Sowiżdżał, A., Bujakowski, W. Evaluation of potential, thermal balance and prospective geological structures for needs of closed geothermal systems (hot dry rocks) in Poland. Warszawa-Kraków, Polish Geological Institute-National Research Institute, 2013. (in Polish)

Yang, W., Lu, P., Cheng, Y. Laboratory investigations of the thermal performance of an energy pile with spiral coil ground heat exchanger. Energy and Buildings, 2016, 128(1): 491-502.

Zhang, W., Qu, Z., Guo, T., et al. Study of the enhanced geothermal system (EGS) heat mining from variably fractured hot dry rock under thermal stress. Renewable Energy, 2019, 143: 855-871.